



Using Ferrocement to Resist Penetration of Hyper-Velocity Objects

M.E. Mohamed^{*}, E.M. Eltehawy[†], I.M. Kamal[†], A.A. Aggour[†]

Abstract: Protective layers of fortified structures are considered key points in resisting missiles. Most of these protective layers are made from plain concrete. Due to the progressive development of military destructive weapons such as hyper-velocity missiles, plain concrete protective layers are not sufficient to resist the effect of hyper-velocity objects. So it is essential to have a new generation of protective layers to able to resist this kind of weapons.

The objective of this paper is to enhance the protective layer material through designing a special concrete mixture with high reliability to resist the penetration of hyper-velocity object. Ferrocement technique is used to enhance the concrete panels' penetration resistance. A parametric study is performed on the effect of changing number of the steel wire mesh layers inside the concrete panels on its penetration resistance. The study in this paper is based on the finite element model verification conducted by M.E. Mohamed et al. using AUTODYN-3D on "Numerical Simulation of Projectile Penetration in Reinforced Concrete Panels" [1].

Also, plain concrete and ferrocement panels' penetration resistance was studied under the effect of hypervelocity objects. This Hyper-velocity projectile was presented in experimental work conducted by Dawson [2]. The main findings of this paper were that there is an enhancement in the penetration resistance for ferrocement panels rather than plain concrete once. Also increasing of steel layers mesh number have slight influence on the penetration resistance of the ferrocement panels.

Keywords: Hyper-velocity, Concrete Panels; Ferrocement; AUTODYN 3D.

1. Introduction

Understanding the response of concrete panels to impact is essential in order to design the fortified structures. When a projectile impacts and penetrates a concrete target, the penetration is accomplished by displacing the target material radially and as a result a tunnel-shaped crater is formed in the target. The target resistance to penetration depends on a number of parameters including the projectile velocity and the relative strength of the projectile and the target. For projectile velocities exceeding 1500 m/s, the penetrator erodes almost completely implying that penetration of a semi-infinite body can be successfully predicted employing the one-dimensional modified hydrodynamic theory of penetration, Tate [4]. The essence of the mechanics of penetration of a solid projectile into a solid target is represented through erosion of the penetrator material in combination with its rigid body motion. This is the framework of this theory.

^{*} Egyptian Armed Forces, Egypt, mamd-sayd07@hotmail.com.

[†] Egyptian Armed Forces, Egypt.

The most common impact phenomena to determine the low limit of the hyper-velocity regime is the complete pulverization of the projectile and target material in the immediate region of the original contact point. The projectile and local target material may be considered fluids when the stresses induced by the impact are many times the materials strength. Thus the principle of fluid mechanics may be used to at least start hypervelocity impact analyses [5]. According to hydrodynamic theory the hydrodynamic (fluid) limit for penetrating concrete is

(P/L) limit = $\sqrt{\rho_p / \rho_t}$ this limit is compared with the erosion rate ($T/\Delta L$) which is the thickness of the target divided by the length loss of the projectile [2]. Where ρ_p is the projectile density and ρ_t is the target density.

For hyper-velocity impact on concrete target penetration depth are proportional to the penetrator's loss of length [6].

For the target material, when the penetrator velocity is fixed, the structure of the plastic flow field in the target defines the extent of the ensuing target material displacements (both the radial and the axial) which in turn determines the size of the resulting crater. Therefore, since the structure of this flow field is controlled primarily by the yield-strength properties of the target, the constitutive behavior of the target material is the principle factor that determines the target's resistance to penetration.

Numerous studies were conducted on behavior of reinforced concrete target subjected to missile impact; studies were mostly focused on concrete properties, and how to prevent excessive local damage and collapse of the target [7-10], that's by enhancement of concrete properties. Different from plain concrete in which mainly the strength dominates its ability of resisting penetration, reinforced concrete may be influenced by both the concrete strength and the amount of reinforcement. In reinforced concrete panels reinforcing mesh is made of about 1 – 2 cm diameter steel bar and the distance between bars is about 10 – 20 cm. Usually 2 – 3 layers of mesh are inserted in concrete panel for reinforcement. Another one of the most important ways to enhance the concrete properties is the ferrocement. Ferrocement is a type of thin-wall reinforced concrete commonly constructed of cement mortar reinforced with closely spaced layers of continuous and relatively small size wire mesh. The typically range of diameter from about 0.4 mm up to about 2.5 mm, and typically the spacing between wire centers ranges from about 10 mm up to about 30 mm. The mesh may be made of metallic or other suitable materials. The fineness of the mortar matrix and its composition should be compatible with the mesh [11].

Ferrocement improves the resistance of the concrete slabs to fragmentation, and increases the ability of the slabs to withstand impact loads [12, 13].

It is clear that the experimental work for hyper-velocity objects is very complicated and costly so, the numerical simulation technique is adopted in paper to study the effect of hyper-velocity objects on the ferrocement models.

This paper employs the explicit dynamic finite element code 3D- AUTODYNE to analyze the behavior of ferrocement model during projectile penetration. The results from the constitutive model RHT that includes strain-rate and damage with a pressure-dependent yield surface shows relatively good agreement with experimental results. The damage contours at the impact and exit surface from the simulation are also consistent with the post-test damage results[14-16].

2. Finite Element Analysis

To study the effect of hyper-velocity objects on concrete, the verified finite element models for plain concrete and ferrocement panels which conducted [1] were used. The hyper-velocity projectile adopted for this study was the projectile with the same properties and velocity as used in Dawson's study [2]. But the length of the used projectile was 187.5 mm which give length / Diameter ratio ($l/d = 30$) as shown in *Figure (1)*. The projectile velocity was 2200 m/sec as in [2].

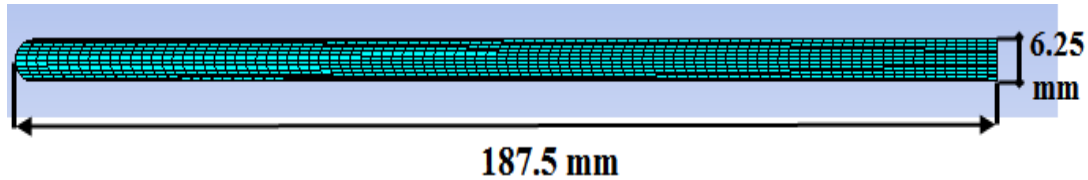


Fig. 1 The geometry of the used projectile ($l/d=30$).

2.1 Description of Finite Element Models

Four finite element models were used to simulate the hyper-velocity concrete penetration. These models were described in *Table (1)*. All material models used in these simulations will be described below, and also the geometry and meshes of all models.

Table 1 The finite element model description

No	Models Name	Description of the Models	No of steel layer	Thick-ness (cm)	Total number nodes	Parts Name	Material
1	Hyper (0)	Plain concrete	-	40	326352	Concrete 1, 2	Conc. 35MPa
						projectile	Tungsten alloy
2	Hyper (1)	Ferrocement one layer	(1) in each face	40	277656	Concrete 1, 2	Conc. 35MPa
						Steel Mesh1-8	STEEL 1006
						projectile	Tungsten alloy
3	Hyper (2)	Ferrocement two layer	(2) in each face	40 cm	325680	Concrete 1, 2	Conc. 35MPa
						Steel Mesh1-8	STEEL 1006
						projectile	Tungsten alloy
4	Hyper (3)	Ferrocement three layer	(3) in each face	40	373704	Concrete 1, 2	Conc. 35MPa
						Steel Mesh1-8	STEEL 1006
						Projectile	Tungsten alloy

2.1.1 Material description

1) Penetrator material

The material model used to simulate the projectile material in all models was (Tungsten alloy) material model [2]. This material model was chosen from the AUTODYN library. The equation of state was *Shock equation of state*, and the strength model was *Johnson Cook strength model*, whereas the failure model was *None* and the erosion model was selected to be *Geometrical strain*. The data defines the penetrator material in the model was chosen from the library and modified, according to the material properties presented by Dawson [2].

2) Target (Concrete) material

The material model used to simulate the plain concrete material this model was (CONC 35MPa) material model. This material model was chosen from the AUTODYN library. The equation of state was *P-Alpha equation of state*, and the strength model was *RHT CONCRETE strength model*, whereas the failure model was *RHT CONCRETE* and the erosion model was selected to be *geometrical strain*. The data defines the concrete material was chosen from the library and modified, according to material properties presented in [3].

3) Steel layer material

The material model used to simulate the steel layer parts material in the model was (STEEL 1006) material model. This material model was chosen from the AUTODYN library. The equation of state was *Linear equation of state*, and the strength model was *Piecewise JC strength model*, whereas the failure model was **None** and the erosion model was selected to be *geometrical strain*. The data defines the steel layer (STEEL 1006) material was chosen from the library and modified, according to material properties presented in [3].

2.1.2 Description of the mesh

Lagrange processor, which described before, has been used in AUTODYN for the analyses. In this thesis two classes of target panels were considered; plain concrete panels, and ferrocement panels. The projectile part and the concrete target parts were divided to elements using as Lagrangian meshes in all models, while the reinforcing steel bars (meshes) were described as beam elements in ferrocement models. All parts were symmetric on $X=0$ planes to reduce the size of the computational domain. The geometry and meshes of the projectile, concrete target and steel mesh, listed in Table 1, will be described below.

1) Projectile mesh

The geometry of the projectile part was defined using a structural Lagrangian mesh. Due to the symmetric conditions of projectile, projectile geometry, which was 6.25 mm diameter and 94.6 mm length, was modeled as a quarter cylinder. It was divided to 7 nodes in the I-direction, 7 nodes in the J-direction and 48 nodes in the K-direction. The total number of element was 2352 elements. This IJK-index is known as a Cartesian co-ordinate system. The projectile part after meshing was filled with its material (Tungsten alloy). Fig. 1 shows the geometry and mesh description for the projectile part.

2) Plain concrete meshes

For plain concrete 40 cm model, targets 1&2 of plain concrete material (Conc.35MPa) were defined using a structural Lagrangian mesh. Due to the symmetric conditions, the geometry of the each part which was square 550 mm side length and 200 mm thickness was modeled as half box. It was divided to 46 nodes in the I-direction, 91 nodes in the J-direction and 41 nodes in the K-direction. The total number of element was 162000 for each part, as same as targets in previous model. Zoning technique was used to refine the meshes in critical region, the element size was 2 X 2 X 5 mm in the impact (maximum stress) region . Each part after meshing was filled with its material (CONC 35 MPa). Fig. 2 shows the geometry and meshes of model plain concrete 40 cm hyper (0).

Each layer from the steel layers was a 500 x 500 mm woven wire meshes of 50 mm square opening and 2.0 mm diameter, these steel layers were used to reinforce the concrete panels from the front and back side. Each steel layer part was defined using 1197 beam element for each layer. Zoning technique was used to refine the mesh in the critical region; the element size was 1 X 1 X 5 mm in the impact (maximum stress) region. Each steel layer part was filled after meshing with its material (STEEL1006). Fig. 4 shows the geometry and meshes of steel layer.

2.2 Finite Element Model Set Up

The initial condition for projectile parts in all models was 2200 m/sec in Z direction where the boundary conditions in all model for all concrete target parts were constant velocity in Y direction $V_y = 0$, the boundary conditions for the back side target were constant velocity in Z direction $V_z = 0$.

Projectile – concrete interaction in all models were achieved using Lagrange/Lagrange interaction.

3. Results

The response of the previous four models, subjected to hyper-velocity objects, was examined and recorded in terms of the following parameters:

- Erosion rate.
- Residual velocity.
- The absorbed kinetic energy.

The results of models were listed in Table 2 and will be discussed in details soon.

Table 2. Numerical simulation result of hyper-velocity penetration resistance

NO	Model Name	Model Disruption	Penetration depth (cm)	Erosion rate ($T/\Delta L$)	Residual Velocity (m/s)	Absorbed K.E.(KJ)
1	Hyper (0)	Plain concrete 40 cm	40	3.66	1724	176.848
2	Hyper (1)	Ferrocement one layer	40	2.303	646.2	236.614
3	Hyper (2)	Ferrocement two layer	40	2.299	634.7	236.618
4	Hyper (3)	Ferrocement three layer	40	2.291	628.9	236.733

3.1 Plain Concrete 40cm (Hyper 0)

- Erosion rate:-

Figure 5 shows the eroded projectile after penetration process.

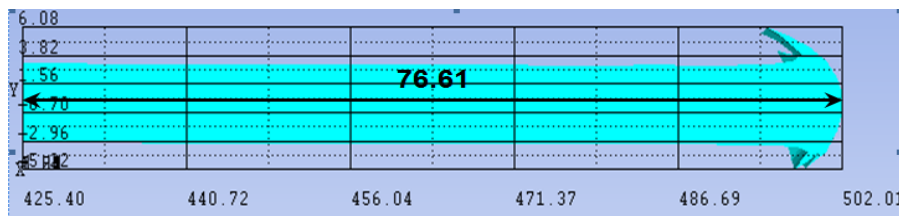


Fig. 5 Projectile after penetration process for model (hyper 0-1).

From Fig. 5 the residual length of the projectile was 76.61 mm and the length loss was 110.89 mm. Then the erosion rate ($T/\Delta L$) was 3.66.

- Residual velocity:-

Figure 6 presents the projectile velocity-time history.

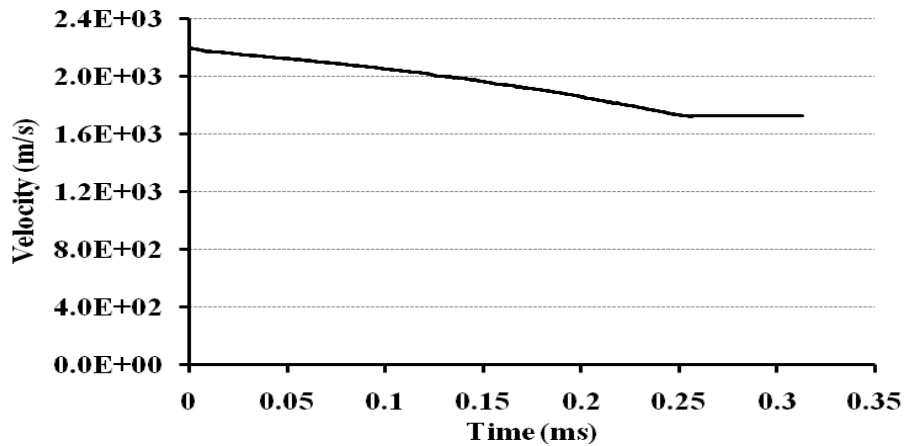


Fig. 6 Projectile velocity-time history for model (hyper 0).

From Figure (6) it is clear that the projectile exist after full perforation with exit (residual) velocity 1724 m/sec.

(c) The absorbed kinetic energy:-

Figure (7) presents the projectile kinetic energy time history.

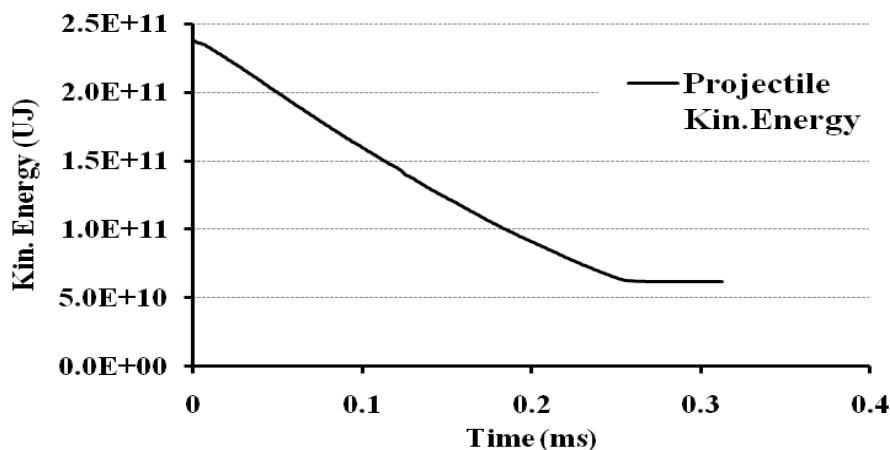


Fig. 7 Projectile kinetic energy time history for model (hyper 0-1).

From Figure (7) the impact kinetic energy was 238.08 KJ and the exit kinetic energy was 61.596 KJ , the absorbed kinetic energy during the penetration process was 176.848 KJ, this energy employed in penetration , the heat generated during the process, and in deformation of the projectile.

3.2 Ferrocement One Layer (Hyper 1)

(a) Erosion rate:-

Figure 8 shows the eroded projectile after penetration process.

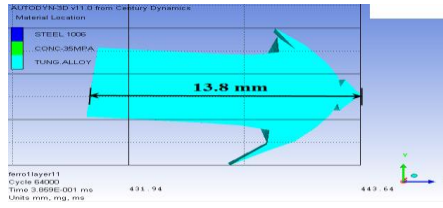


Fig. 8 Projectile after penetration process for model (hyper 1).

From Fig. 8 the residual length of the projectile was 13.8 mm and the length loss was 173.7 mm. Then the erosion rate ($T/\Delta L$) was 2.303.

(b) Residual velocity:-

Figure 9 presents the projectile velocity-time history.

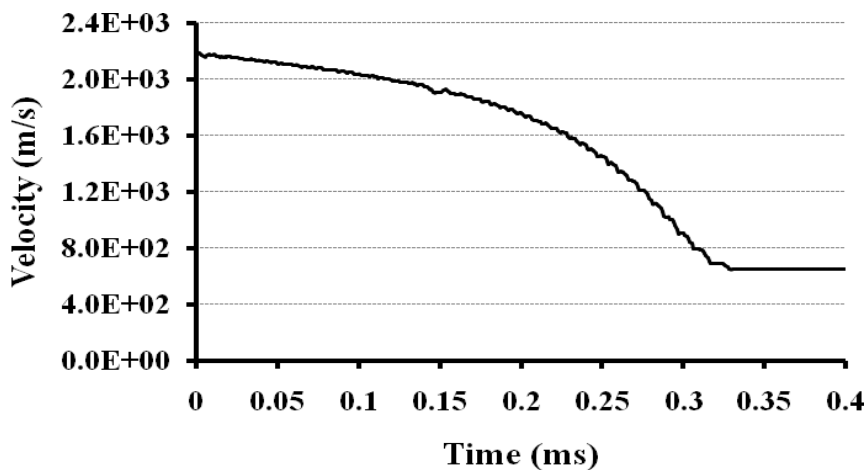


Fig. 9 Projectile velocity-time history for model (hyper 1)

From Fig. 9 it is clear that the projectile exist after full perforation with exit (residual) velocity 646.2 m/sec.

(c) The absorbed kinetic energy:-

Figure 10 presents the projectile kinetic energy time history.

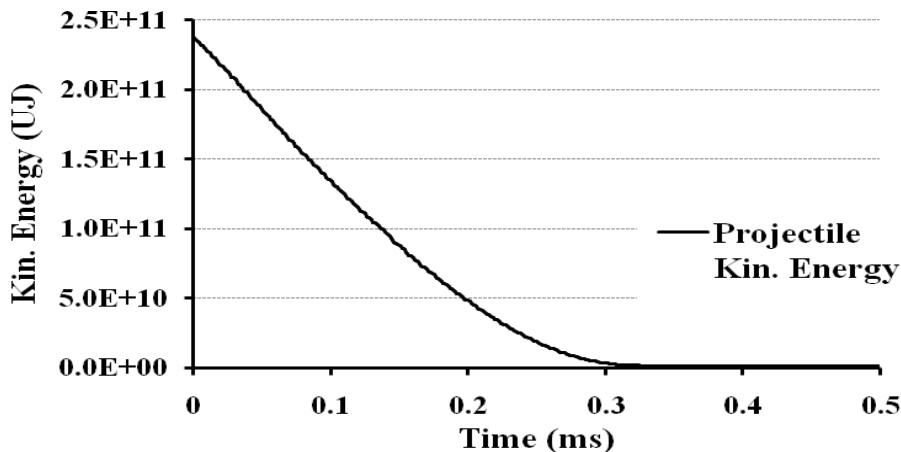


Fig. 10 Projectile kinetic energy time history for model (hyper 1-1).

From Fig. 10, the impact kinetic energy was 238.08 KJ and the exit kinetic energy was 1.466 KJ, the absorbed kinetic energy during the penetration process was 236.614 KJ, this energy employed in penetration, the heat generated during the process, and in deformation of the projectile.

3.3 Ferrocement Two Layer (Hyper 2)

a) Erosion rate:-

Figure 11 shows the eroded projectile after penetration process.

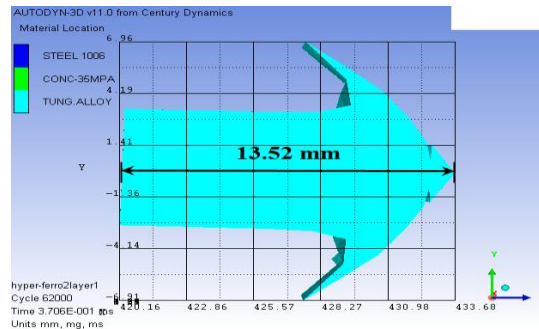


Fig. 11 Projectile after penetration process for model (hyper 2).

From Fig. 11 the residual length of the projectile was 13.52 mm and the length loss was 173.98 mm. Then the erosion rate ($T/\Delta L$) was 2.299.

b) Residual velocity:-

Figure 12 presents projectile velocity-time history.

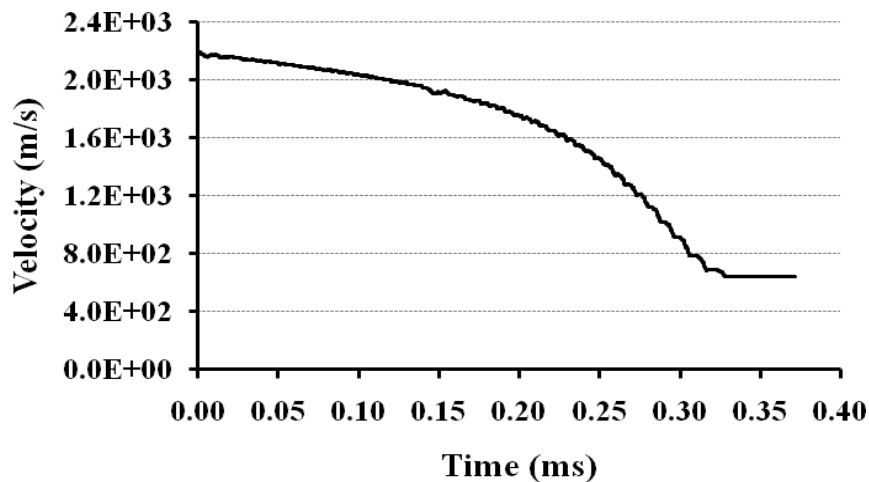


Fig. 12 Projectile velocity-time history for model (hyper 2).

From Fig. 12 it is clear that the projectile exist after full perforation with residual velocity 643.7 m/sec.

c) The absorbed kinetic energy:-

Figure 13 presents the projectile kinetic energy time history.

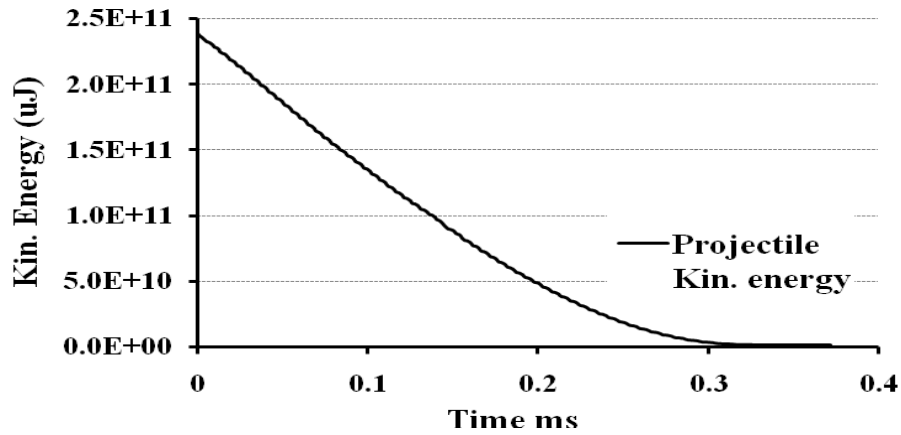


Fig. 13 Projectile kinetic energy time history for model (hyper 2).

From Fig. 13, the impact kinetic energy was 238.08 KJ and the exit kinetic energy was 1.462 KJ, the absorbed kinetic energy during the penetration process was 236.6 KJ.

3.4 Ferrocement Three Layer (Hyper 3)

a) Erosion rate

Figure 14 shows the eroded projectile after penetration process.

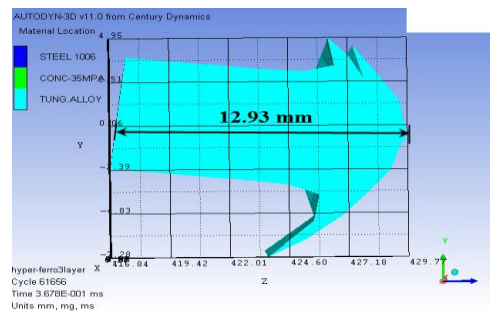


Fig. 14 Projectile after penetration process for model (hyper 3).

From Fig. 14 the residual length of the projectile was 12.93 mm and the length loss was 174.57 mm. Then the erosion rate ($T/\Delta L$) was 2.291.

b) Residual velocity

Figure 15 presents projectile velocity-time history.

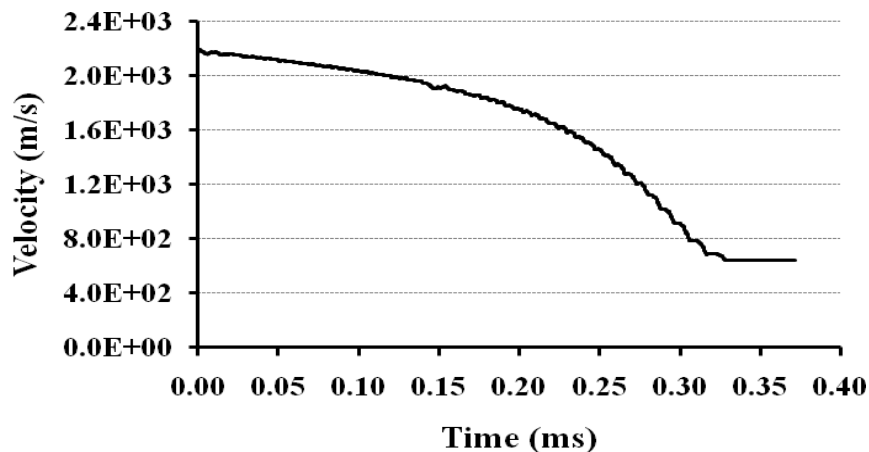


Fig. 15 Projectile velocity-time history for model (hyper 3).

From Fig. (15) it is clear that the projectile exist after full perforation with residual velocity 628.9 m/sec.

c) The absorbed kinetic energy:-

Figure 16 presents the projectile kinetic energy time history.

From Fig. 16 the impact kinetic energy was 238.08 KJ and the exit kinetic energy was 1.347 KJ , the absorbed kinetic energy during the penetration process was 236.733 KJ.

4. Discussion

The penetration resistance of concrete models subjected to hyper-velocity objects was examined in the previous parametric study. In the parametric study, the effect of using ferrocement technique was recorded in terms of the penetration depth, erosion rate, residual velocity, and the absorbed kinetic energy.

4.1 Effect of Using Ferrocement on Erosion Rate

Because the target was relatively thick compared to the projectile diameter, we can assume that the erosion rate $(T/\Delta L) = dP/dL$, where P is penetration. From the hydrodynamic theory (Tate1969) [8], the hydrodynamic limit for tungsten penetrating concrete is (P/L) limit =

$$\sqrt{\rho_p / \rho_t} = 2.74 \text{ for the used concrete.}$$

From the previous results in Table 2 and as discussed before, the following findings were obtained:-

- 1) In case of plain concrete model (hyper 0), the erosion rate was 3.66 which exceed the hydrodynamic limit. That is means the erosion of the projectile is not affected by the strength of the barrier; but in case of using ferrocement in the other models, the erosion rate was about 2.299. This value was less than the hydrodynamic limit which means that the panel strength enhanced and affected on the erosion of the projectile. Using ferrocement reduces the erosion rate by about 37.18 %.
- 2) Increasing number of layers from one layer in (hyper 1) model to three layers in (hyper 3) reduced the erosion rate by 0.33 % which means that increasing number of layers has slight effect on erosion rate.

4.2 Effect of Using Ferrocement on Residual Velocity

From the previous results in Table (2) and as discussed before, the following findings were obtained:

- 1) Using Ferrocement reduced the residual velocity of projectile after penetration from 1724 m/s in case of plain concrete model to 646.2 m/s in case of ferrocement one layer. The reduction was about 62.5 %.
- 2) Increasing the number of layers reduced the residual velocity from 646.2 m/s in case of ferrocement one layer (hyper1-1) to 628.9 m/s in case of ferrocement three layers (hyper 3). The reduction was about 1 % which means that increasing number of layers has slight effect on reducing the residual velocity.

4.3 Effect of Using Ferrocement on Absorbed Kinetic Energy

From the previous results in Table (2) and as discussed before, the following findings were obtained:-

- 1) Using Ferrocement increased the absorbed kinetic energy during the penetration process from 176.848 KJ in case of plain concrete model to 236.614 KJ in case of ferrocement one layer. The increment was about 33.8 %.

2) Increasing the number of layers increased the absorbed kinetic energy from 236.614 KJ in case of ferrocement one layer (hyper1-1) to 236.733 KJ in case of ferrocement three layers(hyper 3-1). The increment was about 0.06 % which means that increasing number of layers has slight effect on the absorbed kinetic energy during the penetration process.

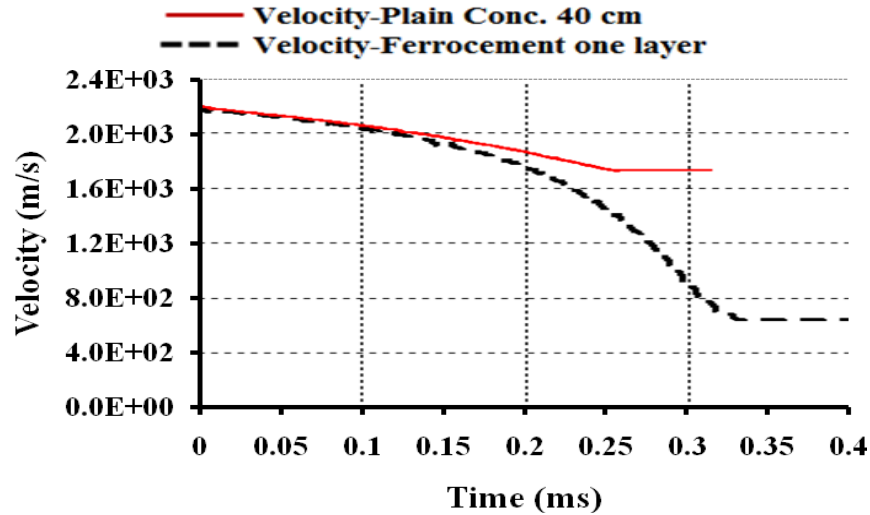


Fig. 17. Enhancement in residual velocity with using Ferrocement.

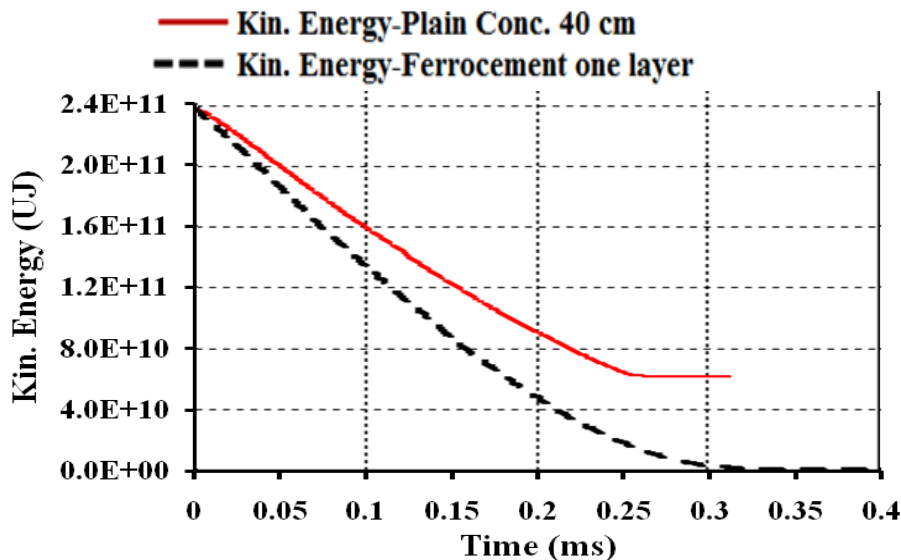


Fig. 18. Enhancement in absorbed energy with using Ferrocement.

5. Conclusions

This paper presents the effect of using ferrocement technique in resisting hyper-velocity objects. The general conclusions derived from analyzing the previous numerical simulation results can be as following:-

- 1) Using Ferrocement enhances the penetration resistance of concrete panels subjected to hyper-velocity impact. That is through increasing the panel strength (which reduce the erosion rate by about 37 %), reduction in residual velocity by about 62.5 %, and increasing the absorbed energy during the penetration process by about 33.8 %.
- 2) Increasing of wire mesh has slight influence on the ferrocement panel's penetration resistance subjected to hyper-velocity impact

6. References

- [1] Mohamed M. E., E.M. Eltehawy, I. M. Kamal, A. A.Aggour, "Numerical Simulation of Projectile Penetration in Reinforced Concrete Panels" *Proceedings of the 13th International Conference on Aerospace Sciences and Aviation Technology, ASAT-13,* May 26-28, 2009.
- [2] Dawson A., S. Bless, S. Levinson, B. Pedersen, and S. Satapathy, "Hypervelocity Penetration of Concrete" *International Journal of Impact Engineering*, p. 1-6, 2008.
- [3] Mohamed M. E., E.M. Eltehawy, I. M. Kamal, A. A.Aggour, "Experimental Analysis of Reinforced Concrete Panels Penetration Resistance" *Proceedings of the 13th International Conference on Aerospace Sciences and Aviation Technology, ASAT-13,* May 26-28, 2009.
- [4] Tate, A., "Further Results in the Theory of Long Rod Penetration" *Journal of Mechanics and physics*, 17, p. 141-150, 1969.
- [5] Macauloy, M., "Introduction to Impact Engineering", Chapman and Hall, USA, 1987.
- [6] Gold, V.M., and C.V. George, "Analysis of the Penetration Resistance of Concrete" *Journal of Engineering Mechanics*, 3, p. 328-337, 1998.
- [7] M.H. Zhang, V.P.W. Shim, G. Lu and C.W. Chew, "Resistance of High-Strength Concrete to Projectile Impact", *Int. J. Impact Eng.*, Vol. 31, pp. 825–841, 2005.
- [8] Avraham N. Dancygier , David Z. Yankelevsky, Chanoch Jaegermann "Response of High Performance Concrete Plates to Impact of Non-Deforming Projectiles" *Int. J. Impact Eng.*, Vol. 34, (2007), pp.,1768–1779.
- [9] P.S. Song, J.C. Wu , S. Hwang , B.C. Sheu "Assessment of Statistical Variations in Impact Resistance of High-Strength Concrete and High-Strength Steel Fiber-Reinforced Concrete" *Cem. Concr. Res.*, Vol.35, pp., 393–399, 2005.
- [10] Mohamed H. Hassoun, "Introducing a New Shape of Steel Fibers and Studying its Effect on the Mechanical Properties of Concrete", M.Sc. thesis, Military Technical College, Cairo, Egypt, 2005.
- [11] ACI Committee 549, "State-of-the-Art Report on Ferrocement", ACI549-R97, in *Manual of Concrete Practice*, ACI, Detroit, p. 26, 1997.
- [12] Shah, S.P and E. Naaman, "Crack Control in Ferrocement and Its Comparison with Reinforced Concrete", *Journal of Ferrocement*, 8, p. 67-80, 2005.
- [13] Abdullah, K., K. Takiguchi, K. Nishimura, and S. Hori, "*Behavior of Ferrocement Subjected to Missile Impact*", *Proceedings of the 17th International Conference on Structural Mechanics in Reactor Technology*, Prague, Czech Republic, p.1-6, August 17–22, 2003.
- [14] Leppänen J., "Concrete Subjected to Projectile and Fragment Impacts Modeling of Crack Softening and Strain Rate Dependency in Tension" *International Journal of Impact Engineering*, 32, p. 1828-1841, 2006.
- [15] Leppänen, J., "Dynamic Behavior of Concrete Structures subjected to Blast and Fragment Impacts", Lic thesis, Chalmers University of Technology, Sweden 2002.
- [16] AUTODYN Explicit Software for Non-linear Dynamics "AUTODYN Electronic Document Library" Multiversions, Century Dynamics Inc., 2005.